



**HAL**  
open science

## Power Frequency Balance in Multi-Generation Smart Grid Systems with V2G option.

Hitesh Datt Mathur, Houria Siguerdidjane, Yogesh Krishan Bhatshvar

► **To cite this version:**

Hitesh Datt Mathur, Houria Siguerdidjane, Yogesh Krishan Bhatshvar. Power Frequency Balance in Multi-Generation Smart Grid Systems with V2G option.. 12th IEEE India International Conference INDECON 2015, Dec 2015, New Delhi, India. 10.1109/INDICON.2015.7443686 . hal-01258654

**HAL Id: hal-01258654**

**<https://centralesupelec.hal.science/hal-01258654v1>**

Submitted on 29 Mar 2020

**HAL** is a multi-disciplinary open access archive for the deposit and dissemination of scientific research documents, whether they are published or not. The documents may come from teaching and research institutions in France or abroad, or from public or private research centers.

L'archive ouverte pluridisciplinaire **HAL**, est destinée au dépôt et à la diffusion de documents scientifiques de niveau recherche, publiés ou non, émanant des établissements d'enseignement et de recherche français ou étrangers, des laboratoires publics ou privés.

# Power Frequency Balance in Multi-Generation Smart Grid System with V2G option

H.D. Mathur,

Department of Electrical and Electronics  
Engineering,  
BITS, Pilani Campus, Pilani, India  
mathurhd@gmail.com

H. Siguerdidjane,

Automatic control department,  
Centrale Supélec, Gif-Sur-Yvette, Cedex,  
France  
Houria.Siguerdidjane@centralesupelec.fr

Y.K. Bhatshvar,

Department of Electrical and Electronics  
Engineering,  
BITS, Pilani Campus, Pilani, India  
yogeshbhatshvar@gmail.com

**Abstract**— In smart grid scenario, penetration of large scale renewable energy sources are increasing rapidly. This causes uncertainty among various power system parameters, mainly frequency in interconnected power system. When automatic generation control (AGC) is not sufficient to manage balance between demand and supply, battery energy storage is considered a viable option for short term active power support in order to bring frequency back to normal. In energy storage possibilities, super conducting magnetic energy storage, ultra-capacitor etc. are primarily discussed. This paper focuses on integrated model of vehicle to grid (V2G) and wind power as an alternative to supply instant power to regulate frequency when system is subjected to sudden perturbation. GA (Genetic algorithm) optimized fuzzy logic controller is used to intelligently suppress frequency and tie-line power oscillations. Results obtained are comprehensively presented and discussed in achieving power-frequency balance. MATLAB/Simulink is used for the simulation purpose.

**Keywords**—Automatic Generation Control; Genetic Algorithm; Vehicle to Grid; Wind Power; Fuzzy Logic Controller

## I. INTRODUCTION

Recently, there has been substantial increase in penetration of renewable sources of energy into electrical grid. Government of most of the countries worldwide are encouraging use of clean and green power in their countries by means of supporting various smart grid projects. This has given impetus to researchers across the globe to give a serious thought to implement a viable solution for reduction in greenhouse gases which are caused by emission of conventional thermal plants and existing vehicles. Policy makers are promoting the use of electric vehicles (EVs) with an option for user to sell electrical power to grid and get benefitted in different means.

According to statistics available, EVs are in idle situation in 90% of the time every day and have sufficient energy to cater to ancillary service requirements particularly frequency regulation in large power system [1-3]. There have been advanced battery technologies and charging infrastructure which is leading to more use of PHEVs (Plugged in hybrid electrical vehicle) and EVs in near future. Therefore, V2G is seen as potential source in frequency regulation [4-7]. Reference [8] has used EVs for secondary frequency modulation and results in decrease in area control error and tie-line deviations. In US, China and India, there are expectations

of large number of EVs on the road as per their government plans [9-12]. Moreover, PHEVs are also being looked as a controllable load for future smart grid [13], [14]. PHEVs are basically charged in the night period as electricity price is cheap during that time [15]. An autonomous distributed V2G control of grid-connected PHEV and EV to the actual frequency measurements in Eastern 50 Hz system and western 60 Hz system of Japan is proposed in [16]. Reference [17] proposes the V2G control based on the average battery SOC deviation control applied to compensate the LFC capacity in the system. Reference [18] concentrates on the autonomous distributed V2G control considering the charging request and battery condition for suppressing the fluctuations of frequency and tie-line power flow in the two-area interconnected power system. The battery SOC is controlled by the SOC balance method. There has been various control strategies implemented in multi-area power system by researchers from conventional control to intelligent control [19-23].

This paper is mainly focusing on understanding different aspects of V2G and wind power inertial support mechanism (WISM) in restructured two area interconnected power system to overcome power-frequency imbalance. EVs are considered in this paper as a sufficiently large energy storage which will cater to power grid when there is need of power in case of sudden rise in demand. Wind power has gained sufficient popularity amongst power generating companies. Apart from supplying electrical power to grid, wind generators are also used to provide inertial support during large and sudden load perturbation. Modeling of V2G and WISM have been done in section II of paper. Controller design is another important aspect presented in the paper. Different intelligent techniques are used in literature for approaching this power system power-frequency balance issue. Fuzzy logic controller with genetic algorithm for optimization is used. The model and strategy are discussed in detail in section III. Section IV presents the simulation results and discussion on different conditions of V2G and Wind power connection in restructured power system. Conclusions are presented in Section V.

## II. SYSTEM MODELING

### A. Mathematical Modelling of Two Area Restructured Power System

The interconnected restructured power system considered has two control areas, each having two generation companies

(GENCOs) and two distribution companies (DISCOs). There are two different models taken for study. In model 1, two reheat thermal units are connected in area-1 and two hydro-based generating units are in area-2 while the two identical thermal units are used in both areas in model 2. Both areas are connected via tie-line for exchange of power in model 1 and 2. DISCOs are operating on the basis of participation matrix [19], [20]. The system parameters are same as used in [20] for thermal and hydro units.

The thermal and hydro unit components are characterized by standard transfer function [20]. In restructured environment, the concept of contract participation factor matrix (CPFM) makes the visualization of contracts. In CPFM, the number of rows indicates the number of GENCOs and the number of columns indicates the DISCOs [24] and sum of all *cpfs* is unity in a column of matrix.

The frequency regulation depends on the control signal composed of tie-line deviation and weighted frequency deviation. It is called area control error (ACE), as shown in (1).

$$ACE_i = \Delta P_{tie,i} + \beta_i \Delta f_i, \quad (1)$$

Where  $\beta_i$  is the frequency bias constant.

$$APFM = \begin{bmatrix} apf_1 & 0 & 0 & 0 \\ 0 & apf_2 & 0 & 0 \\ 0 & 0 & apf_3 & 0 \\ 0 & 0 & 0 & apf_4 \end{bmatrix}. \quad (2)$$

In deregulated environment, within a control area, ACE is again distributed among several GENCOs by coefficients are termed as ACE participation factors (*apfs*). The area participation factor matrix (APFM) is illustrated in (2).

The contracted scheduled loads in DISCOs in area-1 are  $\Delta P_{Ld1\_cont}$  and  $\Delta P_{Ld2\_cont}$  but in area-2 they are  $\Delta P_{Ld3\_cont}$  and  $\Delta P_{Ld4\_cont}$ , as shown in the  $\Delta P_{LD\_cont}$  matrix. The uncontracted local loads in DISCOs in area-1 are  $\Delta P_{Ld1\_uncont}$  and  $\Delta P_{Ld2\_uncont}$  but in area-2 they are  $\Delta P_{Ld3\_cont}$  and  $\Delta P_{Ld4\_cont}$ , as shown in the  $\Delta P_{LD\_uncont}$  matrix [9].

$$\Delta P_{LD\_cont} = \begin{bmatrix} \Delta P_{Ld1\_cont} \\ \Delta P_{Ld2\_cont} \\ \Delta P_{Ld3\_cont} \\ \Delta P_{Ld4\_cont} \end{bmatrix}, \quad \Delta P_{LD\_uncont} = \begin{bmatrix} \Delta P_{Ld1\_uncont} \\ \Delta P_{Ld2\_uncont} \\ \Delta P_{Ld3\_uncont} \\ \Delta P_{Ld4\_uncont} \end{bmatrix}.$$

The total demanded load power  $\Delta P_{LD}$  is represented by (3).

$$\Delta P_{LD} = \Delta P_{LD\_cont} + \Delta P_{LD\_uncont}. \quad (3)$$

Similarly, the contracted generated powers in area-1 are  $\Delta P_{g1\_cont}$  &  $\Delta P_{g2\_cont}$ , but in area-2 they are  $\Delta P_{g3\_cont}$  &  $\Delta P_{g4\_cont}$ , as given in the  $\Delta P_{G\_cont}$  matrix.  $\Delta P_{g1\_uncont}$  &  $\Delta P_{g2\_uncont}$ , are uncontracted generated powers from area-1, but  $\Delta P_{g3\_cont}$  &

$\Delta P_{g4\_cont}$  are uncontracted generated powers from area-2, as given in the  $\Delta P_{G\_cont}$  matrix.

$$\Delta P_{G\_cont} = \begin{bmatrix} \Delta P_{g1\_cont} \\ \Delta P_{g2\_cont} \\ \Delta P_{g3\_cont} \\ \Delta P_{g4\_cont} \end{bmatrix}, \quad \Delta P_{G\_uncont} = \begin{bmatrix} \Delta P_{g1\_uncont} \\ \Delta P_{g2\_uncont} \\ \Delta P_{g3\_uncont} \\ \Delta P_{g4\_uncont} \end{bmatrix}.$$

Contracted generated power by GENCOs,  $\Delta P_{G\_cont}$  is calculated by (4).

$$\Delta P_{G\_cont} = CPFM \cdot \Delta P_{LD\_cont}. \quad (4)$$

Uncontracted generated power by GENCOs,  $\Delta P_{G\_uncont}$  is calculated by (5).

$$\Delta P_{G\_uncont} = APFM \cdot \Delta P_{LD\_uncont}. \quad (5)$$

Therefore, the total generation power by each GENCO at steady state is visualized in the  $\Delta P_G$  matrix, as expressed in (6).

$$\Delta P_G = \Delta P_{G\_cont} + \Delta P_{G\_uncont}. \quad (6)$$

The scheduled tie-line power flow between area-*i* and area-*j* can be represented in (7) and (8).

$$\Delta P_{L,Ai \rightarrow Aj} = \sum_{m=1}^M \sum_{n=1}^N (cpf_{mn} * \Delta P_{Ld(n)_cont}) \quad (7)$$

$$\Delta P_{tieij,sch} = \Delta P_{L,Ai \rightarrow Aj} - \Delta P_{L,Aj \rightarrow Ai}. \quad (8)$$

## B. Mathematical Modeling of Wind power generating system with inertial support mechanism

All areas in developed restructured power system model are connected with a wind power generating unit separately. DFIG model [25] is used for the inertial support to have short term active power supply. The model is simplified with controller is shown in Fig. 1. A one-mass model for the mechanical drive of the turbine is considered. The mechanical power developed by the turbine is given as:

$$P_M = \frac{1}{2} \rho \pi R^2 C_p(\lambda, \beta) v^3 \quad (9)$$

where  $R$  is the rotor radius,  $v$  is the wind speed,  $\rho$  is the air density, and  $C_p$  is the power coefficient of the turbine which depends on the pitch angle,  $\beta$ , and the tip-speed ratio,  $\lambda$ , which is defined by:

$$\lambda = \frac{R \omega_e}{v} \quad (10)$$

where  $\omega_e$  is the rotor speed. The power coefficient is a characteristic of the wind turbine, and for our case, it can be approximated by

$$C_p(\lambda, \beta) = \sum_{i=0}^4 \sum_{j=0}^4 \alpha_{i,j} \beta^i \lambda^j \quad (11)$$

The rotor speed, as well as the pitch angle must be controlled to optimize the amount of power captured by the wind turbine. Thus, a reference speed,  $\omega^*$ , is generated based on the electric power,  $P_e$ , for maximum power tracking and given by (12):

$$\omega^* = -0.67 P_e^2 + 1.42 P_e + 0.51 \quad (12)$$

Then, the generator speed is controlled by a PI controller that has as output the value  $P_{\omega}^*$ , given by:

$$P_{\omega}^* = K_p(\omega^* - \omega_e) + K_I \int (\omega^* - \omega_e) dt \quad (13)$$

To support the frequency variation in the grid, the so-called inertial control must be added to system. This controller adds to the power reference output signal given by:

$$P_f^* = -K_{df} \frac{d\Delta f}{dt} - K_{pf} \Delta f \quad (14)$$

where  $K_{df}$  and  $K_{pf}$  are constants and must be chosen as weights to the frequency deviation derivative and frequency deviation respectively. This signal can increment the system inertia, supporting the frequency variation indirectly. Thus, the total active power reference for our turbine must be calculated as follows:

$$P_{\omega}^* = P_{\omega}^* + P_f^* \quad (15)$$

The penetration level is possible to change for study and variation is studied extensively in [20] but it is considered to be 30% for all simulation purpose in this paper.

### C. Mathematical Modeling of Vehicle to Grid (V2G) System for frequency regulation

The EVs participation in AGC is from a broader perspective is used in developing mathematical model of EVs. Secondary frequency regulation is primarily accomplished by control action with area control error as input to controller. EVs for vehicle to grid process need to be modeled by keeping in view of change in frequency and AGC control signal. Communication channels between AGC and EVs is simplified and designed as an aggregated EVs model for secondary frequency control. The State of charge (SOC) of electrical vehicle is noted at every instant to have the correct accumulated capacity of all available EVs for frequency regulation. Therefore, EVs are basically used as reserve capacity to cater at the time of sudden demand in power system and this would be case in peak hours during a load cycle. The inputs are controller output and change in frequency to aggregated model of EVs for V2G which is represented by a first order transfer function.  $K_{EV}$  and  $T_{EV}$  are frequency characteristic of aggregated EVs and V2G time constant respectively. There values are calculated by power capacity of area and maximum change in frequency. The values of these parameters are considered as 10 and 0.1 respectively for all

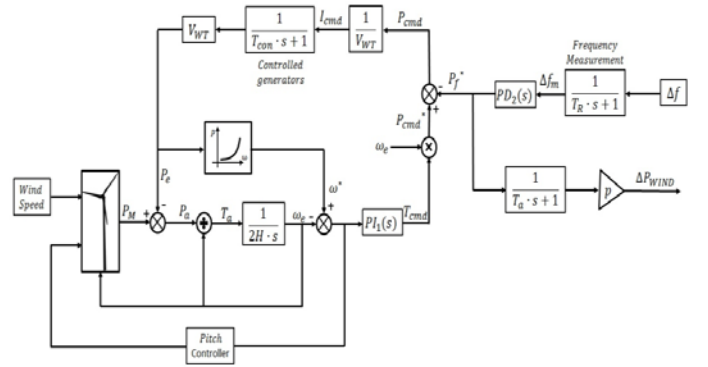


Fig. 1: Simplified block diagram of wind turbine simulation purpose. The other parameters are same as given in [20].

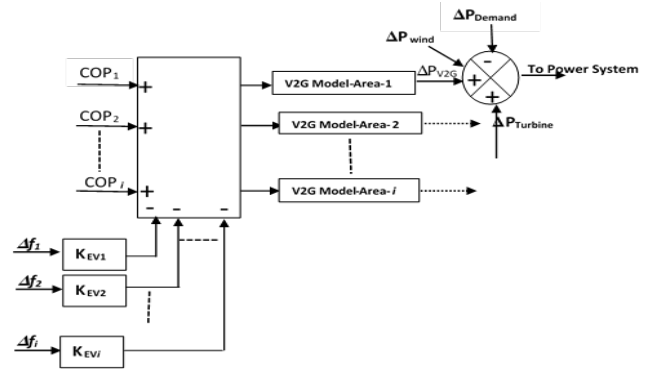


Fig 2: An integrated model with V2G for AGC in multi-generating system

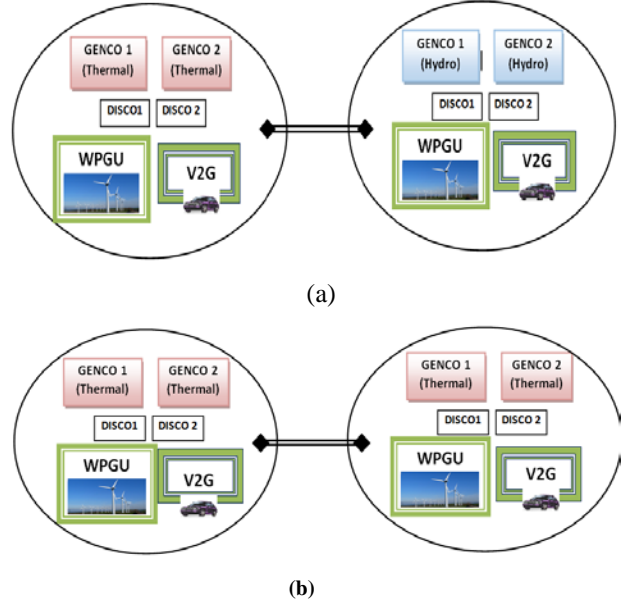


Fig. 3: (a) Model 1 with Thermal and Hydro Units in area-1 and area-2 respectively (b) Model 2 with Thermal Units in area-1 and area-2

The integrated model for AGC in multi-area interconnected power system is shown in Fig. 2, where  $COP_1, COP_2, \dots, COP_i$  and  $\Delta f_1, \Delta f_2, \dots, \Delta f_i$  are controlled input for conventional AGC and change in frequency from area-1, area-2 and  $i^{th}$  area

respectively. Transfer function representing V2G model is given by (16),

$$\Delta P_{EV} = \frac{1}{T_{EV}s+1} \quad (16)$$

An aggregated model of EVs represented by a single transfer function for a particular area is used and has a simplified communication process between AGC and EVs. The prime purpose of having EVs grouped together that they represent a virtual large energy storage plant with a sufficient capacity to support AGC at the time of peak demand or sudden demand during the course of power supply at any other time.

TABLE I RULE BASE FOR FLC

		ΔACE						
		VVL	VL	L	Z	H	VH	VVH
ACE	VVL	VVL	VVL	VL	VL	L	L	Z
	VL	VVL	VL	VL	L	L	Z	H
	L	VL	VL	L	L	Z	H	H
	Z	VL	L	L	Z	H	H	VH
	H	L	L	Z	H	H	VH	VH
	VH	L	Z	H	H	VH	VH	VVH
	VVH	Z	H	H	VH	VH	VVH	VVH

VVH: Very Very High, VH: Very High, H: High, Z: Zero, L: Low, VL: Very Low, VVL: Very Very Low

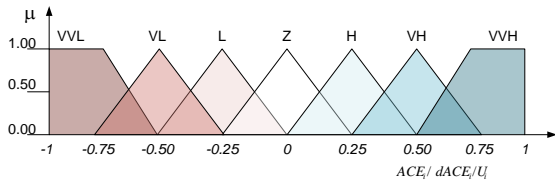


Fig. 4: MF's Distribution within defined variable range

### III. PROPOSED CONTROL STRATEGY

In this paper, an optimized control strategy has been implemented. First model which is shown in Fig. 3 (a), and model 2 in Fig. 3 (b) are used for simulations. A fuzzy logic controller, where PI controller parameters as well as range of variables are optimized using GA. The perturbations are represented by the demand raised from DISCOs and basically it is step signal of 0.05 pu. In the recent times, fuzzy logic controller (FLC) has gained popularity in control system applications in uncertain and nonlinear systems. In complex and multi-variable power system, conventional control methods may not give satisfactory solutions. On the other hand, FLCs are more robust and more reliable in solving a wide range of control problems. Fuzzy logic is a systematic and easier way to implement control algorithm for uncertain and indefinite models in engineering. The FLC modeling consists of three steps as fuzzification, formation of fuzzy control rule base and defuzzification [23]. The control actions of a FLC are described by some set of linguistic rules and these are obtained from experience or trial and error, but this way does not lead towards optimum results. In order to achieve optimized results,

FLC is done using powerful optimization tool i.e. GA in a systematic way.

Seven membership function (MF) have been used to explore best performance as shown in Fig.4. The FLC is designed based on MISO type. The first input is  $ACE_i$  and other one is derivative of  $ACE_i$  ( $dACE_i/dt$ ) which justifies of PI controller implementation. In Fig. 5,  $K_e$  and  $K_{ce}$  are scaling factors for both input variable respectively and  $K_p$  and  $K_i$  are the proportional and integral gains. Whereas,  $U_i$  is a crisp value and  $u_i$  is a control signal for the system.

$$u_i = -K_p U_i - K_i \int U_i dt \quad (17)$$

Initially for each variable, MF's distribution are kept same. MF specifies the degree to which a given input belongs to set or a function that defines how each point in the input space is mapped to a degree of membership between 0 and 1. MF's distribution for  $ACE_1$  is within [-0.5 0.5],  $dACE_1$  is within [-0.1 0.1] and  $U_1$  is within [-0.5 0.5] for FLC controller for area-1 and for area-2 MF's distribution for  $ACE_2$  is within [-0.5 0.5],  $dACE_2$  is within [-0.1 0.1] and  $U_2$  is within [-0.1 0.1] for FLC controller for area-2.

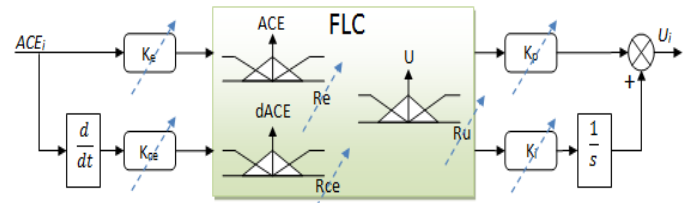


Fig. 5: MISO Fuzzy Logic controller

Table I presents the rules for FLC used in designing the controller. In rule base 49 rules are designed to get the response.

### IV. SIMULATIONS AND DISCUSSION

Simulations are performed on two different models as discussed earlier. Results obtained are using MATLAB/Simulink. The dynamic parameters of frequency response have been critically analyzed to justify the controller actions on different case studies. There have been four cases with each model type which makes total 16 simulation graphs of change in frequency in area-1 and area-2 respectively.

#### A. Case 1 (No Wind Power and V2G Power Penetration):

The disturbance is subjected in both areas and results obtained are given in Fig. 6 and 7. Oscillatory response is observed in model 1 with high setting time and peak overshoot. The main reason of having such response is interconnection of thermal and hydro units. There is difference in their time constants which results in sustained oscillations for sufficiently longer time. On the other hand, when model 2 is considered, there is stable response as both the areas are similar and acting simultaneously to perturbation. All responses in model 2 will have same peak overshoot and settling time for this reason.

**B. Case 2 (With Wind Power and No V2G Power Penetration):**

In second case, wind power inertial support is connected in all areas along with conventional AGC system. Since both areas are equipped with wind power generating units (WPGU), this is leading to short term active power support to some extent and managing to minimize oscillatory behavior of frequencies in both areas in model 1 particularly. Model 2 already has smooth responses but immediate power demand is met by WPGU leading to lesser overshoot as compared to previous case. Graphical results are shown in Fig. 6 and 7 for both models.

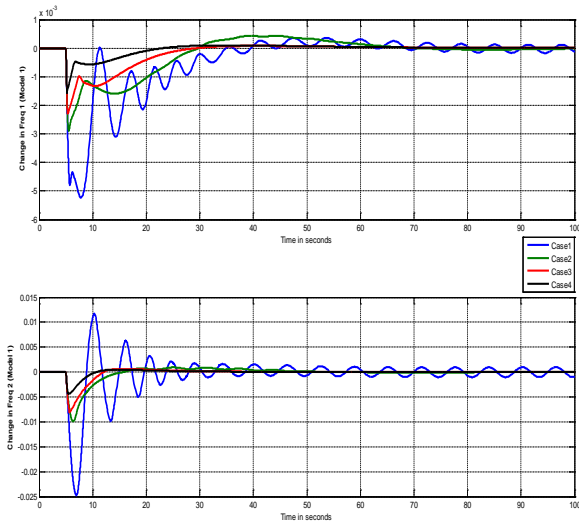


Fig. 6: Frequency deviations in area-1 and area-2 for model 1 in all cases

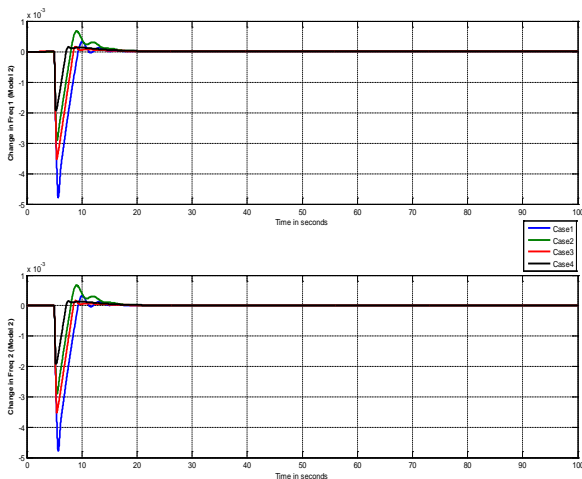


Fig. 7: Frequency deviations in area-1 and area-2 for model 2 in all cases

**C. Case 3 (Without Wind Power and With V2G Power Penetration):**

In smart grid era, where possibilities of micro grids are being discussed amongst researchers with V2G power penetration. These results in an interconnected power system

with V2G effect should be considered encouraging in terms of frequency regulations. In this particular case, only V2G is incorporated in both areas of power systems under study. The responses shown in Fig. 6 and 7 are justifying the presence of having bulk vehicle power storage in new power system age. This is alone capable enough to have substantial improvement in dynamic parameters of response as clearly visible in graphs. The major reason here is fast acting converters and a small response time of overall model of V2G support system.

**D. Case 4 (With Wind Power and V2G Power Penetration):**

This case represents an integrated approach to handle power system frequency regulation challenge. The integration of WPGUs and V2G support system is connected in both areas. Keeping the same perturbation for obtaining comparative analysis, this case results in finest form. In both models, not only peak overshoot and settling time are reduced but also a smooth and oscillation free responses are achieved. This integration has its justification in smart grid system because smart grid focuses on mainly clean power inputs into the grid. Both of them (WPGUs and V2G) are indeed foremost choices for power engineers. There are always issues associated with both of them because of their technical complexity in design for practical purpose, but nevertheless, this suits best for frequency regulations aspect. Results with integrated model in place are shown in Fig. 6 and 7 for model 1 and 2 respectively.

All results are also presented in Table II. Observing all results for model 1, it may be concluded that by simply putting V2G into system, there is 47% decrease in peak overshoot and 62% in settling time from case 1 to case 4 in area-1 only while if area-2 is considered, new values are 33% and 20% of their earlier values. Integrated model of V2G and WPGUs leads to highly encouraging results i.e. peak overshoot and settling time in area-1 are 30% and 39 % of their initial values.

If model 2 is considered where both areas are similar, all results of different cases are same for area-1 and area-2. Peak overshoot and settling time are considerably reduced i.e. new values are 38% and 7% of their earlier values. Finally, it is recommended that V2G should be considered as a viable and suitable option for critical aspect of modern day power system i.e. frequency regulation. This is obvious to say that the practical power plants will have slightly higher dynamic parameters with such controller as there will be more non-linearities into the electro-mechanical system.

**Table II** COMPARATIVE ANALYSIS

Case	Area	Model 1 (Thermal-Hydro)		Model 2 (Thermal-Thermal)	
		Peak Overshoot (Hz)	Settling Time (s)	Peak Overshoot (Hz)	Settling Time (s)
1	1	-0.005313	28.83	-0.004925	8.99
	2	-0.024734	97.40	-0.004925	8.99
2	1	-0.003022	24.41	-0.002987	9.73
	2	-0.009908	39.02	-0.002987	9.73
3	1	-0.002573	18.73	-0.003569	8.07
	2	-0.008089	19.50	-0.003569	8.07
4	1	-0.001616	11.72	-0.001913	6.68
	2	-0.004345	9.52	-0.001913	6.68



## V. CONCLUSION

An integrated V2G and WPGUs model is presented in paper for automatic generation control in restructured power system. A newly developed V2G model represents an aggregated V2G where vehicles are assumed to be available for bulk power supply for short term. This is justified and validated with simulation results presented. Power system engineers come across the situations of sudden rise in demand quite often. This solution is a win-win situation for both customers and power companies. Two different models of power system are used for a comprehensive analysis of effect of wind power and V2G power. Wind power generating units are modeled with inertial support which is crucial at the time of sudden load requirement in power system because thermal and hydro generators lose their kinetic energy to support additional demand which is undesirable. Despite the fact that associated power management system will have to be quick in transferring information through a secured and robust communication channels, V2G has capability of changing power scene in days to come.

## REFERENCES

- [1] F. Baccino, M. Marinelli, S. Massucco, and F. Silvestro, "Low voltage microgrid under islanded operation: Control strategies and experimental tests," Power Generation, Transmission, Distribution and Energy Conversion (MEDPOWER 2012), 8th Mediterranean Conference on, pp.1-7, Cagliari, 1-3 Oct. 2012.
- [2] Y. Zoka, R. Tonoda, Y. Mashima, Y. Sasaki, and N. Yorino, "An on-demand control system for demand and supply control of small independent power grids," Universities Power Engineering Conference (UPEC), 2012 47th International, pp.1-6, London, 4-7 Sept. 2012
- [3] Wenqi Tian; Jinghan He; Liyong Niu; Weige Zhang; Xiaojun Wang; Zhiqian Bo, "Simulation of vehicle-to-grid (V2G) on power system frequency control," Innovative Smart Grid Technologies - Asia (ISGT Asia), 2012 IEEE , vol., no., pp.1.3, 21-24 May 2012
- [4] Ota, Y.; Taniguchi, H.; Nakajima, T.; Liyanage, K.M.; Baba, J.; Yokoyama, A., "Autonomous distributed V2G (vehicle-to-grid) considering charging request and battery condition," Innovative Smart Grid Technologies Conference Europe (ISGT Europe), 2010 IEEE PES , vol., no., pp.1.6, 11-13 Oct. 2010
- [5] K. Shimizu, T. Masuta, Y. Ota, and A. Yokoyama, "Load Frequency Control in Power System Using Vehicle-to-Grid System Considering the Customer Convenience of Electric Vehicles", in Proc. 2010 International Conference on Power System Technology (PowerCon)
- [6] K. M. Liyanage, A. Yokoyama, Y. Ota, T. Nakajima, H. Taniguchi, "Impacts of Communication Delay on the Performance of a Control Scheme to Minimize Power Fluctuations Introduced by Renewable Generation under Varying V2G Vehicle Pool Size", in Proc. 2010 IEEE SmartGridComm.
- [7] A. Brooks, E. Lu, D. Reicher, C. Spirakis, and B. Wehl, "Demand Dispatch", IEEE Power & Engineering Magazine, Vol.8, Issue.3, pp.20-29, May. 2010.
- [8] Almeida, P.M.R.; Lopes, J.A.P.; Soares, F.J.; Vasconcelos, M.H., "Automatic Generation Control operation with electric vehicles," Bulk Power System Dynamics and Control (iREP) - VIII (iREP), 2010 iREP Symposium , vol., no., pp.1.7, 1-6 Aug. 2010
- [9] W. Su and M.-Y. Chow, "Performance evaluation of an EDA-based large-scale plug-in hybrid electric vehicle charging algorithm," IEEE Trans. Smart Grid, vol. 3, no. 1, pp. 308–315, Mar. 2012.
- [10] Y. Cao, S. Tang, C. Li, P. Zhang, Y. Tan, Z. Zhang, and J. Li, "An optimized EV charging model considering TOU price and SOC curve," IEEE Trans. Smart Grid, vol. 3, no. 1, pp. 388–393, Mar. 2012.
- [11] Ministry of Power, Government of India, "Smart Grid Vision and Roadmap for India" August 12, 2013
- [12] Vachirasricirikul, S.; Ngamroo, I., "Robust LFC in a Smart Grid With Wind Power Penetration by Coordinated V2G Control and Frequency Controller," Smart Grid, IEEE Transactions on , vol.5, no.1, pp.371,380, Jan. 2014
- [13] A.Yokoyama, "Smarter grid I," IEEJ J., vol. 30, no. 2, pp. 94–97, 2010.
- [14] A. Yokoyama, "Smarter grid II," IEEJ J., vol. 30, no. 3, pp. 163–167, 2010.
- [15] M. Takagi, K. Yamaji, and H. Yamamoto, "Power system stabilization by charging power management of plug-in hybrid electric vehicles with LFC signal," in Proc. 2009 IEEE Veh. Power Propulsion Conf., pp. 822–826.
- [16] Y. Ota, H. Taniguchi, T. Nakajima, K.M. Liyanage, and A. Yokoyama, "An autonomous distributed vehicle-to-grid control of grid-connected electric vehicle," in Proc. 2009 IEEE Ind. Inf. Syst. Conf., pp. 414–418.
- [17] T. Masuta and A. Yokoyama, "Supplementary load frequency control by use of a number of both electric vehicles and heat pump water heaters," IEEE Trans. Smart Grid, vol. 3, no. 3, pp. 1253–1262, Sep. 2012.
- [18] Y. Ota, H. Taniguchi, T. Nakajima, K. M. Liyanage, J. Baba, and A. Yokoyama, "Autonomous distributed V2G (vehicle-to-grid) satisfying scheduled charging," IEEE Trans. Smart Grid, vol. 3, no. 1, pp. 559–564, Mar. 2012.
- [19] Yogesh Krishan Bhatshvar, Hitesh Datt Mathur, Houria Siguerdidjane & Surekha Bhanot, "Frequency Stabilization for Multi-area Thermal-Hydro Power System Using Genetic Algorithm-optimized Fuzzy Logic Controller in Deregulated Environment, Electric Power Components and Systems", 43:2, pp. 146-156, 2015
- [20] Y.K. Bhatshvar, H.D. Mathur and Houria Siguerdidjane, "Study of Impact of Wind Power Generating System Integration on Frequency Stabilization in Multi-area Power System with Fuzzy Logic Controller in Deregulated Environment" Vol. 9, Issue 1, Frontiers in Energy, pp. 7-21, 2015.
- [21] Bhatt, P., Roy, R., and Ghoshal, S.P., "Optimized multi area AGC simulation in restructured power systems," Int. J. Elect. Power Energy Syst., Vol. 32, No. 4, pp. 311–322, 2010.
- [22] Panda, S., and Yegireddy, N.K., "Automatic generation control of multi-area power system using multi-objective non-dominated sorting genetic algorithm-II," Int. J. Elect. Power Energy Syst., Vol. 53, pp. 54–63, 2013.
- [23] Çam, E., and Kocaarslan I., "Load frequency control in two area power systems using fuzzy logic controller," Energy Convers. Manag., Vol. 46, No. 2, pp. 233–243, 2005.
- [24] Tan W, Zhang H, Yu M. Decentralized load frequency control in deregulated environments. International Journal of Electrical Power & Energy Systems, 2012, 41(1): 16–26
- [25] B. Boukhezzer, H. Siguerdidjane, "Nonlinear control with wind estimation of a DFIG variable speed wind turbine for power capture optimization", Energy Conversion and Management, Volume 50, Issue 4, April 2009, Pages 885-892

## APPENDIX:

### A. Parameters of Hydro Thermal System Investigated:

$$P_{r1}=P_{r2}=2000\text{MW}; K_{p1}=K_{p2}=120; T_{p1}=T_{p2}=20; R_1=R_2=2.4; T_{12}=0.545; T_w=1; T_t=0.3; T_{g1}=0.08; T_{g2}=0.02; T_f=5; R_t=0.38; R_p=0.05; \beta=0.425; a_{12}=1;$$

### B. Parameters of Wind Turbine Investigated:

$$H=4.64; pAr=2*0.00159; Kb=56.6; Tr=0.1; Ta=0.2; Tc=0.2; Kp=1.5; Ki=0.15;$$

### C. Parameters of V2G System Investigated:

$$T_e=1; u_e=0.025; del_e=0.01; E_{max}=0.95; E_{min}=0.80; E=0.90; P_{max}=200/1000;$$